Journal of Marine Research, 49, 1–19, 1991

Journal of
MARINE RESEARCH

Volume 49, Number 1

Separation and recirculation of the North Brazil Current

by Scott A. Condie[1,2]

ABSTRACT

The North Brazil Current separates from the French Guiana coast in the western tropical North Atlantic and a portion of the flow retroflects to form a recirculation zone known as the Demerara Anticyclone. The remainder of the North Brazil Current continues northwestward to join the Guiana Current. This part of the flow may be particularly significant, since it carries a cross-gyre transport of heat and mass from the tropical Atlantic into the subtropical gyre. An extension of the recirculation model of Cessi (1988), in which a quasi-geostrophic flow was driven by potential vorticity anomalies along a boundary, has been used to investigate dynamics relevant to the separation and recirculation of the North Brazil Current. Unlike that of Cessi, the present model is two dimensional and consists of two recirculating gyres driven only by the western boundary current potential vorticity distribution. The recirculation zones were much smaller than those predicted by one dimensional models and since most of the streamlines passed through a diffusive boundary layer there was no evidence of homogenization of the potential vorticity field. The influence of diffusivity, boundary forcing and boundary orientation were considered. The western boundary layer was similar to a Munk layer over most of the parameter range investigated. Since the boundary forcing diffused into the interior, the meridional and zonal dimensions of the inertial part of the recirculation both had a weak power law dependency on the boundary forcing and diffusivity. When the western boundary was not aligned with the planetary vorticity gradient, westward drift distorted the shape of the recirculation.

1. Introduction

In recent years it has become clear that classical models, in which western boundary currents close the circulation within ocean gyres (for example Veronis,

1. Department of Oceanography, Old Dominion University, Norfolk, Virginia, 23529, U.S.A.
2. Present address: School of Oceanography WB-10, University of Washington, Seattle, Washington, 98195, U.S.A.

1973) are in many respects inadequate. In particular, a number of western boundary current systems, such as the North Brazil Current, the Somali Current (Philander and Delecluse, 1983) and the Agulhas Current (Ou and Ruijter, 1986), transport water between neighboring gyres. In the case of the North Brazil Current (NBC), significant quantities of mass and heat are carried from the Atlantic equatorial gyre into the subtropical gyre. Csanady (1987) referred to this western boundary current cross-gyre exchange as 'leakage' and suggested that it might play a critical role in the global heat budget of the oceans.

The flow fields in the leakage region of the NBC are particularly complex. Ship drift observations by Richardson and McKee (1984), drifting buoy tracks reported by Molinari (1983) and Richardson and Reverdin (1987) and satellite images by Muller-Karger *et al.* (1988) indicate that a portion of the flow crosses gyres into the Guiana Current, while the remainder separates from the coast and recirculates to form the Demerara Anticyclone. Near its southern extremity, the recirculation also feeds fluid into the North Equatorial Counter Current. Hence, the Demerara Anticyclone acts as a "distributor" for three major currents—the NBC, the Guiana Current and the North Equatorial Counter Current.

A reasonable picture of the flow pattern in the Demerara Anticyclone region, consistent with the above observations, can be obtained from the isotherm depth field derived from AXBT surveys by Bruce and Kerling (1984). The flow field is represented schematically in Figure 1. The South Equatorial Current flows into the NBC south of the Demerara anticyclone. Farther north the NBC separates from the coast and meets the North Equatorial Current at a stagnation point (Csanady, 1990). A portion of the flow returns westward to the coast to form the coastal cyclone or trough and then continues on into the Guiana Current. The remainder retroflects southward to form the Demerara anticyclone and eventually becomes the eastward flowing North Equatorial Counter Current.

This flow field is further complicated by its seasonality. In boreal winter the North Equatorial Counter Current is extremely weak and the cyclonic gyre shinks zonally into a cyclonic eddy structure. The strength of the coastal cyclone may also decrease during this period, although further observational confirmation is required. A number of estimates have been made for the volume transports associated with the retroflection and leakage processes. These are summarized by Csanady (1990) who concluded that the best estimates to date correspond to retroflection of $15 \times 10^6 m^3 s^{-1}$ and leakage of $5 \times 10^6 m^3 s^{-1}$ in boreal summer (Aug–Oct) and retroflection of $3 \times 10^6 m^3 s^{-1}$ and leakage of $4 \times 10^6 m^3 s^{-1}$ in boreal winter (Feb–April). However, there still exists a large degree of uncertainty in these figures and their dependence on the dynamics of the two gyres is relatively unknown.

From a primitive equation general circulation model of the tropical Atlantic, Philander and Pacanowski (1986) examined the seasonal variability in the tropical Atlantic. They were able to reproduce a numer of important features including the

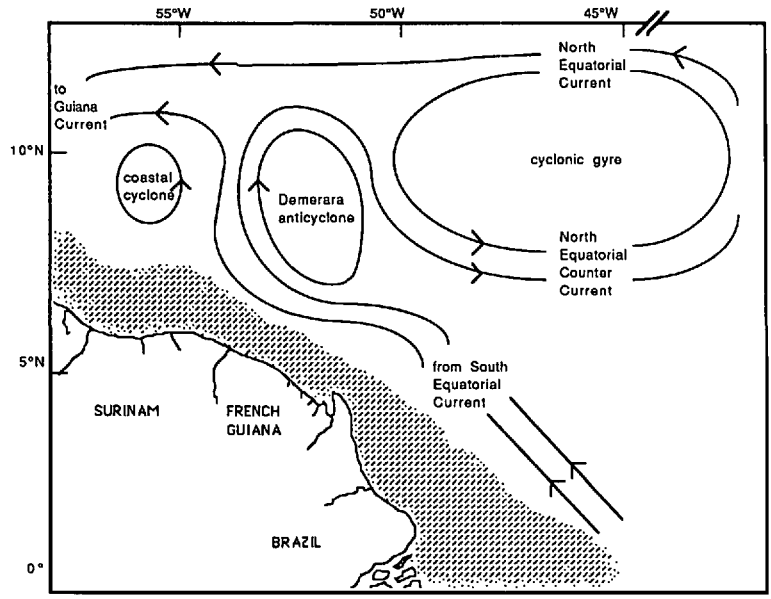

Figure 1. The large scale flow pattern in the western equatorial Atlantic during boreal summer. In boreal winter the North Equatorial Counter Current is very weak and the summer cyclonic gyre shrinks into a large eddy.

retroflection of the NBC to form the Demerara anticyclone and some leakage into the Guiana current. However, serious discrepancies between ship drift data and the model have been reported in the region of the NBC (Richardson and Philander, 1987). In particular, the velocities near the coast were overestimated by a factor of two and the coastal cyclone was absent. The coastal cyclone is a persistently strong feature and is difficult to explain since there are no obvious sources of cyclonic vorticity.

Why the NBC should separate from the coast around 8N is another important question. Local wind stress has little effect on the current and surfacing of the thermocline (as occurs near Cape Hatteras where the Gulf Stream separates) has not been observed. However, hydrographic and current observations by Flagg *et al.* (1986), suggest that there exists a significant potential vorticity discrepancy between the intruding equatorial water and the local subtropical gyre water. Csanady (1985) developed a model of the NBC by proposing that the northern high potential vorticity fluid blocks the intruding NBC. The purely inertial theory predicted a stagnation point somewhere along the coast and it was proposed that leakage occurred past this point due to dissipation.

The major questions we would like to address in this paper are: (i) what factors control the size and strength of the Demerara Anticyclone and (ii) what makes the NBC separate from the coast? The model is quite successful in addressing (i) and

suggests some potentially important aspects of (ii). Although these questions are concerned with the western tropical North Atlantic, the results of the study may have implications for other recirculation zones.

2. The model

Unlike the Gulf Stream system, isopycnal surfaces in the NBC show no tendency to surface. This excludes the use of results from a number of previous models which assume isopycnal surfacing (e.g. Parsons, 1969; Veronis, 1973; Cessi, 1990) and suggests that a quasi-geostrophic formulation would be more appropriate. The model is further simplified by noting that the thermocline beneath the shallow Atlantic tropical surface water drops in temperature from 25°C to 15°C, over a depth of only 50 meters (Merle and Arnault, 1985). This results in a relatively large deformation radius and there is little tendency for the Demerara recirculation to extend below the thermocline. This again contrasts with the Gulf Stream recirculation which has a large barotropic component. These characteristics of the NBC indicate that a one and a half layer model, consisting of a shallow active upper layer overlying a deep passive layer, is particularly appropriate for this region.

The flow in the model is driven entirely by the potential vorticity distribution at the western boundary (which deviates from the planetary value). The boundary forcing is communicated to the fluid by diffusion of potential vorticity. This crudely simulates the transport of anomalous potential vorticity fluid from remote latitudes by the western boundary current. A similar approach has been used previously to study the Gulf Stream recirculation. Cessi *et al.* (1987) developed a barotropic model of this feature, which was later extended to include a second active layer (Cessi, 1988). The principle difference between this study and those of Cessi and her co-workers is that we are particularly concerned with the zonal extent of the recirculation (which for the NBC is less than the meridional scale). This was not addressed by Cessi whose boundary distribution of potential vorticity was independent of longitude. Ierley and Young (1988) introduced zonal dependence into a similar barotropic model by including nonuniform forcing at the northern boundary of the gyre. Although the recirculation appeared more realistic, the zonal length scale of the flow was in part determined by the northern boundary conditions, rather than free jet dynamics.

The zonal problem can be addressed by considering two gyres, which may or may not be symmetrical depending on the application. We need then only specify forcing along the western boundary with all other boundary vorticity values set at the planetary value. With the boundary conditions set as shown in Figure 2, the forcing can be specified entirely in terms of the potential vorticity anomaly in the northwest (southwest) corner of the southern (northern) gyre. This system has the additional

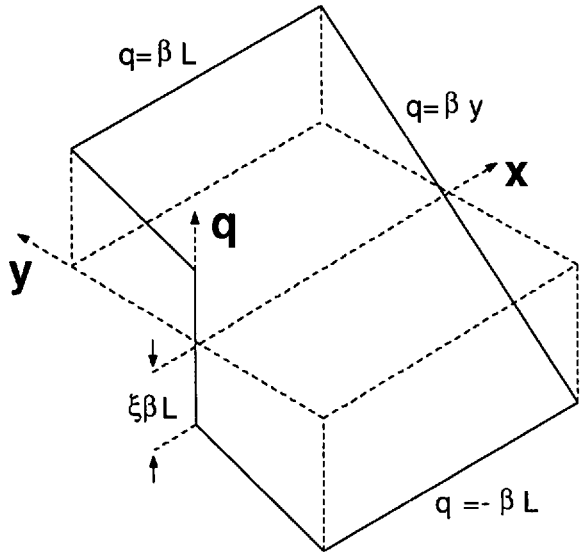

Figure 2. The boundary distribution of potential vorticity. All of the forcing is along the western boundary and can be specified in terms of a single parameter ξ.

advantage, that it gives some insight into the conditions required for the western boundary current to separate from the coast.

3. Formulation

The standard quasi-geostrophic equations for a one and a half layer ocean on a beta plane, with dissipation via lateral potential vorticity diffusion are:

$$\frac{\partial q}{\partial t} + J(\psi, q) = \kappa \nabla^2 q, \tag{1}$$

where q is the potential vorticity, ψ is the streamfunction and κ is the diffusivity. The potential vorticity is defined by

$$q = \nabla^2 \psi - \frac{f_0^2}{g'H}\psi + \beta y, \tag{2}$$

where g' is the reduced gravity, H is the characteristic depth of the upper layer, f_0 is the planetary vorticity at mid-latitude and β is the planetary vorticity gradient. The domain covering the two gyres is $0 < x < 2L$, $-L < y < L$ where x is eastward and y is northward. The streamfunction boundary conditions are,

$$\psi(x, \pm L) = \psi(0, y) = \psi(2L, y) = 0. \tag{3}$$

We begin by considering the simple symmetrical forcing case

$$q(x, \pm L) = \pm \beta L, \tag{4a}$$

$$q(2L, y) = \beta y, \tag{4b}$$

$$\begin{aligned} q(0, y) &= \beta[(1 - \xi)y - \xi L], \quad y < 0, \\ &= \beta[(1 - \xi)y + \xi L], \quad y > 0, \end{aligned} \tag{4c}$$

as illustrated by Figure 2. Solutions for these boundary conditions will be described in Section 5a, while forcing more relevant to the NBC will be considered in Section 5c.

Relations (1) to (4) can be conveniently nondimensionalized according to;

$$(x, y) = L(x', y'), t = t'/\beta L, q = q'\beta L, \psi = \psi'\beta L^3. \tag{5}$$

Dropping the primes from the dimensionless variables, the quasi-geostrophic potential vorticity equation then takes the form,

$$\frac{\partial q}{\partial t} + J(\psi, q) = K\nabla^2 q, \tag{6}$$

with

$$q = \nabla^2\psi - F\psi + y. \tag{7}$$

The strength of the diffusion is determined by $K = \kappa/L^3\beta$, while the Froude number $F = f_0^2 L^2/g'H$ is the ratio of the length scale of the gyre to the deformation radius squared. The boundary conditions (3) and (4) take the nondimensional forms

$$\psi(x, \pm 1) = \psi(0, y) = \psi(2, y) = 0, \tag{8}$$

and

$$q(x, \pm 1) = \pm 1, \tag{9a}$$

$$q(2, y) = y, \tag{9b}$$

$$\begin{aligned} q(0, y) &= [(1 - \xi)y - \xi], \quad y < 0, \\ &= [(1 - \xi)y + \xi], \quad y > 0, \end{aligned} \tag{9c}$$

within the nondimensional domain $0 < x < 2$, $-1 < y < 1$. Values of dimensional parameters relevant to the western tropical North Atlantic are listed in Table 1.

4. Review of one-dimensional solutions

Before proceeding with the full numerical solution, we will briefly review the one-dimensional analytical solutions of Cessi (1988) and calculate their predictions for conditions relevant to the NBC. As noted in the previous section, this is not a particularly appropriate model for the Demerara Anticyclone whose zonal dimension is smaller than its meridional dimension. However, it is worth considering as a limit to the more general two dimensional case and as a useful point of comparison.

Table 1. Dimensional parameters for the western tropical North Atlantic.

Dimensional quantity	Symbol	Value
Gyre scale	L	1000 km
Upper layer depth	H	160 m
Reduced gravity	g'	2.5×10^{-2} m s^{-2}
Planetary vorticity	f_0	2.5×10^{-5} s^{-1}
Planetary vorticity gradient	β	2.2×10^{-11} m^{-1} s^{-1}
Diffusivity	κ	5.0×10^{2} to 1.0×10^{4} m^2 s^{-1}
Deformation radius	$(g'H)^{1/2}/f_0$	80 km
Munk layer thickness	$(\kappa/\beta)^{1/3}$	28 to 77 km

In the one dimensional limit, conservation of potential vorticity along streamlines implies that,

$$q(\psi) = \frac{\partial^2 \psi}{\partial y^2} - F\psi + y. \tag{10}$$

Boundary conditions which prescribe continuity of the streamfunction and velocity are,

$$\psi(0) = \psi(\pm\lambda) = 0. \tag{11}$$

and

$$\frac{\partial \psi}{\partial y}(\pm\lambda) = 0, \tag{12}$$

where λ is the nondimensional meridional dimension of the two symmetrical gyres. The boundary condition for q on both the eastern and western boundaries is given by Eq. (9c). In the limit of small diffusion, the potential vorticity within closed streamlines will be homogenized to a constant value (Rhines and Young, 1982). Assuming that homogenization extends to the edge of the gyre (so that the potential vorticity there is discontinuous[3]) Cessi *et al.* (1987) showed that the homogenized value is simply $q(\psi) = \xi$. Solving (10) and (11) then yields an equation for the zonal velocity in the active layer,

$$-\frac{\partial \psi}{\partial y} = -\frac{1}{F}\left\{1 + F^{1/2}\xi \sinh(F^{1/2}y) - F^{1/2} \cdot \left(\frac{\xi \cosh(F^{1/2}\lambda) + (\lambda - \xi)}{\sinh(F^{1/2}\lambda)}\right)\cosh(F^{1/2}y)\right\}, \tag{13}$$

3. Marshall and Nurser (1986) studied a recirculating gyre with a continuous potential vorticity distribution. However, this problem can only be solved analytically by neglecting relative vorticity which leads to a solution with discontinuous velocity at the edge of the gyre.

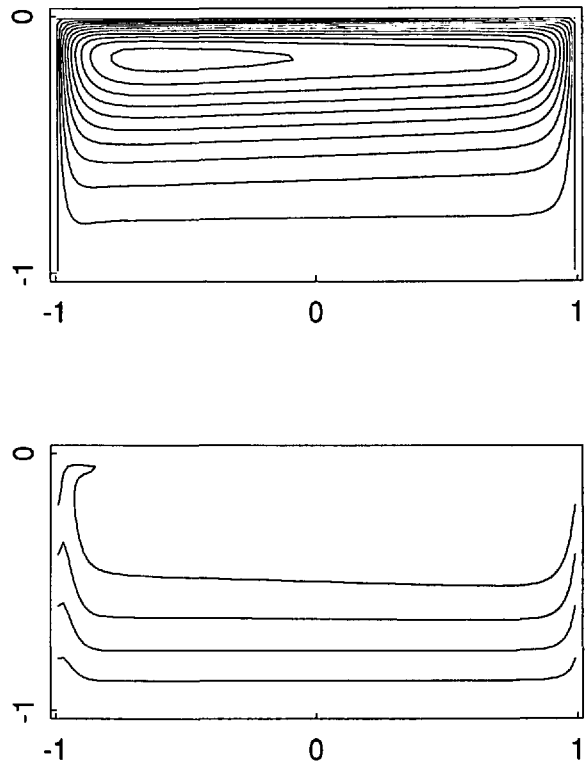

Figure 3. The non-dimensional streamfunction (contour interval 2×10^{-4}) and potential vorticity (contour interval 0.2) in the southern anticyclonic gyre for the one-dimensional problem. The diffusivity was $K = 1 \times 10^{-4}$ and the boundary forcing $\xi = 0.5$.

while the lower layer of depth H_L will have zero velocity provided,

$$\frac{H_L}{H} > -1 + F^{1/2}\left(\frac{\xi \cosh(F^{1/2}\lambda) + (\lambda - \xi)}{\sinh(F^{1/2}\lambda)}\right). \tag{14}$$

Combining (12) and (13) then yields,

$$F^{1/2}\xi = \sinh(F^{1/2}\lambda) - F^{1/2}(\lambda - \xi)\cosh(F^{1/2}\lambda). \tag{15}$$

which relates the size of the recirculation to the forcing. The reader is referred to Cessi (1988) for a more detailed derivation of these results.

Taking an example in which $\xi = 0.5$ and $F = 150$, Eq. (15) predicts that $\lambda = 0.58$ and Eq. (13) gives mid-gyre nondimensional velocities around 3×10^{-3}. Indeed, when Eqs. (6) and (7) are solved numerically with boundary conditions independent of x (as in Cessi *et al.*, 1987 and Cessi, 1988), the results give a homogenized region and velocities close to these predictions. This can be seen from Figure 3 which shows the numerical solution for both the steamfunction and potential vorticity fields in the southern gyre. The main discrepancy from the theory occurs within the outer rim

region where diffusion is significant. Here there is finite flow but no homogenization, which allows the potential vorticity to make a continuous transition to the planetary value.

For the Demerara Anticyclone $F = 150$ and, since intruding western NBC water is of equatorial origin, ξ is close to one (Csanady, 1985). Eq. (13) gives a velocity around 7×10^{-3} or 15 cm s^{-1}, which seem reasonable, although there are no published observations available for a direct comparison. Eq. (14) implies that no motion will be induced in the lower layer provided $H_L/H > 11.2$, which requires only that $H_L >$ 1800 m. However, relation (15) suggests that the recirculation should fill the basin, (i.e. $\lambda \geq 1$) provided $\xi \geq 0.92$. As expected this does not compare well with ocean observations which suggest λ does not exceed 0.3. This discrepancy between the one-dimensional model and observations of the NBC indicates that zonal variations play an important role in the Demerara Anticyclone dynamics and that a two dimensional model is warranted.

5. Two dimensional solutions

The complete two dimensional problem as defined in Section 3 was examined with the aid of a numerical solution. Eq. (6) was integrated by splitting the advection-diffusion operator (time splitting) and using an explicit scheme for the advection term combined with an alternating direction implicit (ADI) scheme for the diffusion term. Eq. (7) was solved at each time step using over-relaxation methods. In all runs shown here a 100 × 100 grid was used which was sufficient to adequately resolve boundary layers. Each experiment was allowed to run for at least one diffusion time L^2/κ (K^{-1} in nondimensional time). The effects of dissipation (K), forcing (ξ) and coastline orientation were considered. Other parameters were held constant at values appropriate for the western tropical North Atlantic (see Table 1).

a. Dissipation and boundary forcing. The effects of varying the diffusivity were examined with the boundary forcing kept at a value of $\xi = 1$. Beginning with relatively high values, the diffusivity was reduced to a point where numerical instabilities became problematic. In Figure 4, the streamfunction and potential vorticity fields are given for a range of diffusivities. At the highest value of K (Fig. 4a) the recirculation extends over the meridional extent of the basin and is most intense along the western boundary and at the border between the two gyres. The high diffusivity ensured that the flow was nearly linear and subsequently there is little distortion of the potential vorticity field from the planetary gradient, beyond that dictated by the boundary conditions. In runs 4b to 4d, a boundary layer and a separate recirculating interior are distinguishable. The distortion of the potential vorticity field associated with nonlinearity can be observed throughout the flow region and is particularly evident in the recirculating interior. However, there is little evidence of homogenization of the potential vorticity field. This contrasts strongly

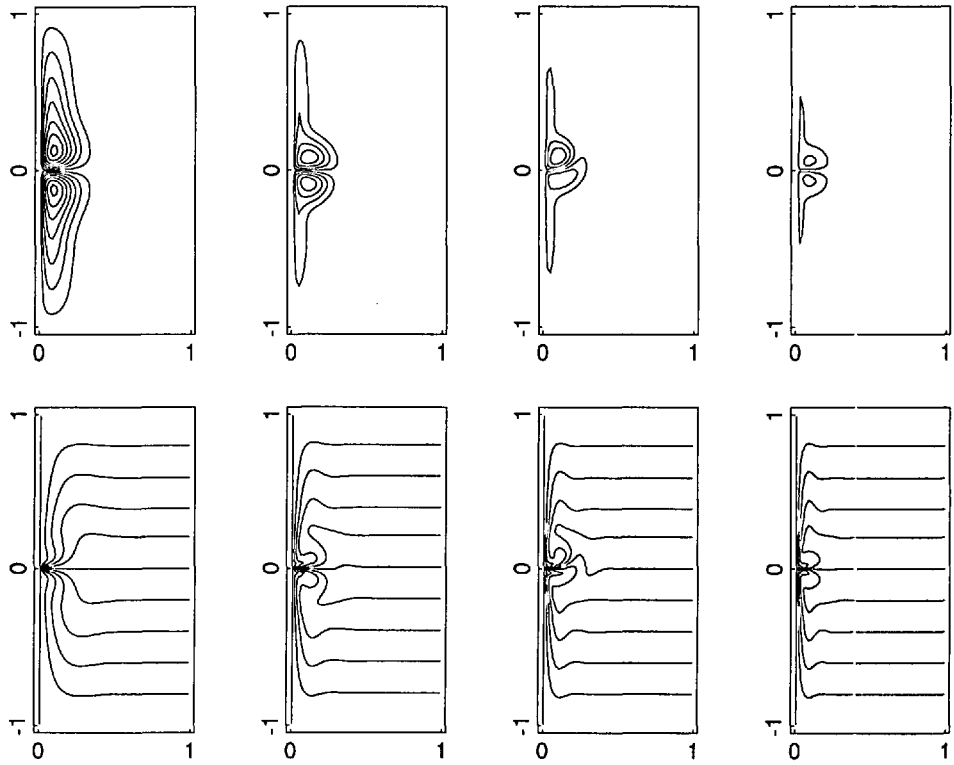

Figure 4. The streamfunction (contour interval 2×10^{-4}) and potential vorticity (contour interval 0.2) in the two-dimensional problem for a range of dissipation levels. The forcing in each case was $\xi = 1$, while the diffusivities and Reynolds numbers for the recirculating part of the flows were (a) $K = 5 \times 10^{-4}$ and $Re = 0.7$, (b) $K = 1 \times 10^{-4}$ and $Re = 8.3$, (c) $K = 0.5 \times 10^{-4}$ and $Re = 9.9$, and (d) $K = 0.25 \times 10^{-4}$ and $Re = 14$. There appears to be some persistent residual time dependency in flow (c). Only the western half of the basin is shown.

with the one dimensional case, as can be seen by comparing Figures 3 and 4b which have the same diffusivities (but different boundary forcing).

Figures 5a to 5c show changes in the streamfunction and potential vorticity as the boundary forcing parameter was reduced from $\xi = 1.0$ to 0.2 with the diffusivity constant at $K = 5 \times 10^{-5}$. As the Reynolds number fell, the recirculation shrunk in size and strength, as did the meridional extent of the boundary current. It should be noted however, that the zonal and meridional scales within the interior remained nearly equal throughout. When ξ fell to a value of 0.2, the recirculation tended to lose its identity within the western boundary layer. At this point there was only very limited distortion of the potential vorticity field.

The one-dimensional solution in Figure 3 and the two dimensional solution in Figure 5b have the same western boundary forcing. A comparison shows that the velocities are similar, but the length scales of the flow are dramatically different, even

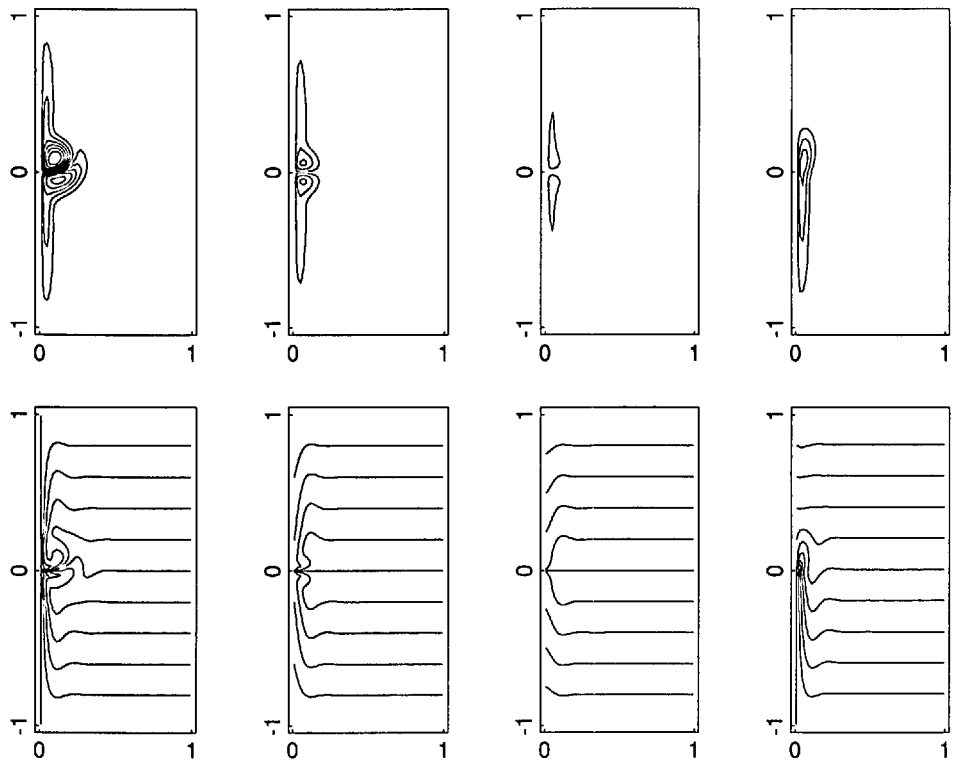

Figure 5. The steamfunction (contour interval 1×10^{-4}) and potential vorticity (contour interval 0.2) for a range of boundary forcing. In each case the diffusivity was $K = 0.5 \times 10^{-4}$, while the first three flows correspond to (a) $\xi = 1.0$ and $Re = 9.9$, (b) $\xi = 0.5$ and $Re = 5.4$, (c) $\xi = 0.2$ and $Re = 1.9$. Flow (d) had $\xi = -1.0$ in the southern half of the basin and no forcing in the north. Again only the western half of the basin is shown.

in the meridional direction. As a second example, if the boundary forcing is increased to $\xi = 1$, the potential vorticity is homogenized over the entire basin in the one-dimensional model. This is in strong contrast to the relatively small two-dimensional recirculation zone in Figure 5a. The differences arise because the one dimensional case is strongly influenced by the northern and eastern boundary conditions, which both act as vorticity sources. The two dimensional recirculation on the other hand, is dependent on the vorticity stored in the free jet after it leaves the western boundary. Another important difference between the one and two dimensional models is the apparent absence of potential vorticity homogenization in the latter. This again relates back to the very limited size of the inertially dominated zone. If the size of the recirculation is not very much greater than the boundary layer thickness, then nearly every streamline must pass through the boundary layer and homogenization cannot occur.

b. Scaling of the two dimensional problem. The numerical solutions indicate that the flows consist of a western boundary current attached to an interior return flow. These two regions may be governed by quite different dynamics. This can be best described in terms of the Reynolds number, defined here by

$$Re = \frac{\delta \psi_{max}}{\lambda K}, \tag{16}$$

where δ is the zonal length scale of the flow and ψ_{max} is the maximum value of the streamfunction. When the Reynolds number is small the diffusive term dominates the potential vorticity equation and the flow is generally of little oceanographic interest.

For a higher Reynolds number flow, the diffusive term may be balanced by the nonlinear term. For boundary forced circulation, this balance ensures that the western boundary layer thickness will scale as,

$$\delta_B \sim \frac{\lambda_B K}{\psi_{max}}, \tag{17}$$

where subscript B denotes the western boundary layer. Since the stretching term tends to be subdominant in the parameter range of interest, $\nabla^2\psi \approx \xi$ within the boundary layer, so that,

$$\psi_{max} \sim \xi \delta_B^2. \tag{18}$$

We would also expect that,

$$\lambda_B \sim \xi, \tag{19}$$

so that relation (17) yields the nondimensional form of the Munk (1950) boundary layer thickness,

$$\delta_B \sim K^{1/3}, \tag{20}$$

which is independent of the forcing parameter. Relation (20) is the result of most practical interest. However, combining (18) and (20) gives

$$\psi_{max} \sim \xi K^{2/3}, \tag{21}$$

which is particularly useful since it can be tested numerically without the rather arbitrary selection of a characteristic boundary layer thickness.

At large Reynolds numbers, the nonlinear term dominates. The one dimensional flows described in Section 4 fall into this category. Although the nature of the forcing in the two dimensional model ensures that diffusion will always be important in the western boundary layer, a purely inertial balance may be appropriate in regions of the flow which extend into the interior. Here nonlinearity can induce distortion of the potential vorticity field, so that potential vorticity is approximately conserved

along streamlines (i.e. $q \approx q(\psi)$). The potential vorticity definition (7) then gives,

$$\nabla^2\psi + y = g(\psi), \tag{22}$$

where $g(\psi) = q(\psi) + F\psi$. The actual form of this function is determined in the boundary layer as suggested by Ierley and Young (1983). Relation (22) states that as the recirculating fluid moves southward along streamlines in the interior, changes in the planetary vorticity are largely balanced by changes in the relative vorticity. This then implies that,

$$\lambda_I\delta_I^2 \sim \psi_{max}, \tag{23}$$

where the subscript I denotes interior scales. However, ψ_{max} is set in the boundary layer in accordance with relation (21), so that,

$$\lambda_I\delta_I^2 \sim \xi K^{2/3}. \tag{24}$$

If $\lambda_I \ll \lambda_B$, then vorticity changes within the recirculation are relatively small. This implies that the meridional and zonal dimensions of the recirculation are comparable, so that

$$\lambda_I \sim \delta_I \sim \xi^{1/3}K^{2/9}. \tag{25}$$

Formation of an inertial region whose dimensions are given by (25) requires firstly that $Re \gg 1$, and secondly that the recirculation extends beyond the diffusive boundary layer. However, the latter condition can be expressed in the form,

$$\delta_I/\delta_B \sim Re^{1/3} > 1. \tag{26}$$

This indicates that the first condition should generally be sufficient to ensure that some of the recirculation is inertial.

The dynamical balance operating in the numerical solutions (Figs. 4 and 5) were determined by comparison with the above scalings. We begin by using relation (21) to test if the western boundary layer satisfied a nonlinear-diffusive balance. ψ_{max} is plotted as a function of $\xi K^{2/3}$ in Figure 6 for all the runs described above. This supports the hypothesis that a Munk scaling is appropriate in the boundary layer over most of the parameter range. A linear fit to the numerically generated data indicates that $\psi_{max} = 0.38\xi K^{2/3}$ for $Re > 1$. The only run which is not consistent with this scaling corresponds to Figure 4a with $Re = 0.7$, for which a purely diffusive balance is appropriate.

Careful comparison of the streamlines and potential vorticity fields in Figures 4 and 5 suggest that a purely inertial balance with potential vorticity conservation holds over a limited region of a number of the flows. The scaling derived for this regime (Eq. 25) was tested by plotting the zonal scale of the recirculation δ_I against the quantity $\xi^{1/3}K^{2/9}$ (Fig. 7). For this purpose δ_I was taken to be the separation of the midpoint of the recirculation (i.e. the location of ψ_{max}) and the most easterly point of

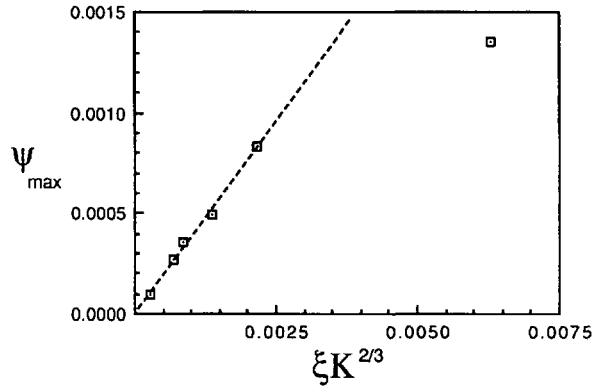

Figure 6. A graph of ψ_{max} vs. $\xi K^{2/3}$ for runs corresponding to Figures 4a-d and 5a-c. The slope of the fitted curve is 0.38.

the streamline $\psi = 1 \times 10^{-4}$. The plot indicates that the scaling is appropriate over a surprisingly large part of the parameter range investigated. This suggests that only a relatively small region of the flow (probably the mid-latitude jet) needs to be purely inertial for the size of the recirculation to be determined by an inertial balance. As expected the scaling is not relevant to the diffusive regime where $Re < 1$ and there is also a tendency for it to fail at the smallest value of $\xi^{1/3}K^{2/9}$. The latter corresponds to Figure 5c where the recirculation is almost entirely submerged in the western boundary layer ($\delta_I/\delta_B = 1.7$) and $Re \sim 1$. We can conclude that the inertial scaling is consistent with the majority of the runs such that $\delta_I = 2.2\xi^{1/3}K^{2/9}$ for $Re > 5$.

c. Non-symmetrical forcing and coastline orientation. The observations described in the introduction show that the vorticity anomaly associated with the Demerara

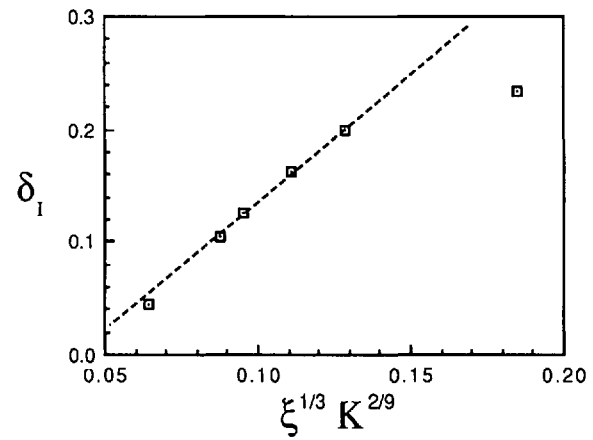

Figure 7. A graph of δ_I vs. $\xi^{1/3}K^{2/9}$ for the same runs as in Figure 6. The slope of the fitted curve is 2.2.

Anticyclone is considerably larger than that associated with the coastal cyclone. The effect of nonsymmetrical forcing of the two recirculation zones was therefore considered. We began with the extreme case of no forcing in the north (i.e. $\xi = -1$ for $y < 0$ and $\xi = 0$ for $y > 0$) shown in Figure 5d. Clearly no cyclone formed under these circumstances and the Reynolds number was much reduced compared to the symmetrical forcing case. The interesting aspect of this flow is therefore the location of the separation point where the boundary current left the coast. The flow passed the point $y = 0$ without separation, despite the step in potential vorticity. The only effect of the step was to reduce the magnitude of the anticyclonic vorticity by increasing the current width and decreasing the shear vorticity. Eventually, the boundary current slowed down and underwent a frictionally dominated separation with the entire flow restricted to the boundary layer. It therefore appears that cyclonic relative vorticity may have initiated the inertial separation in the earlier examples. This proposal will be discussed futher below.

The orientation of the coastline to the planetary vorticity gradient may also be an important factor in the separation and recirculation process. In keeping with our interest in the NBC, a coastline orientated to the northwest was considered. Figure 8 shows three cases in which the forcing in the north was reduced from $\xi = 1$ to 0.2, while the southern forcing was kept constant at $\xi = -1$. With symmetrical forcing (Fig. 8a) the flow field was fairly similar to that produced along a meridional coastline (Fig. 5a) and the dynamical balances essentially the same. However, the misalignment of the western boundary and the planetary vorticity gradient allowed the flow pattern to propagate westward on the beta plane. This caused elongation of the cyclonic gyre, compression of the anticyclonic gyre and introduced weak secondary circulation patterns. If the coastline orientation angle had been increased so that the forcing was located on the southern boundary, then the problem would have been equivalent to that of Ierley and Young (1988). We would, therefore, expect that an increase in the angle between the coast and the planetary vorticity gradient in our model would result in further expansion of the cyclonic gyre to the west and contraction of the anticyclonic gyre into the diffusive boundary layer.

When the boundary forcing in the north was reduced (Fig. 8b), the anticyclonic southern recirculation began to dominate. The inertia of the anticyclonic flow, coupled with westward propagation, carried the flow northwestward around the offshore side of the weaker cyclonic recirculation. The absence of any interior forcing ensured that the streamlines soon closed on themselves rather than continuing northwestward. However the flow pattern does suggest that more realistic forcing could result in leakage of fluid in this direction. When the northern forcing was further reduced (Fig. 8c), the strength of the cyclonic gyre fell so that $Re \sim 1$. The southern gyre then failed to separate at the point where the boundary forcing changed sign. Instead, the weak cyclonic gyre was advected to the northwest, where frictionally dominated separation of the anticyclonic flow occurred.

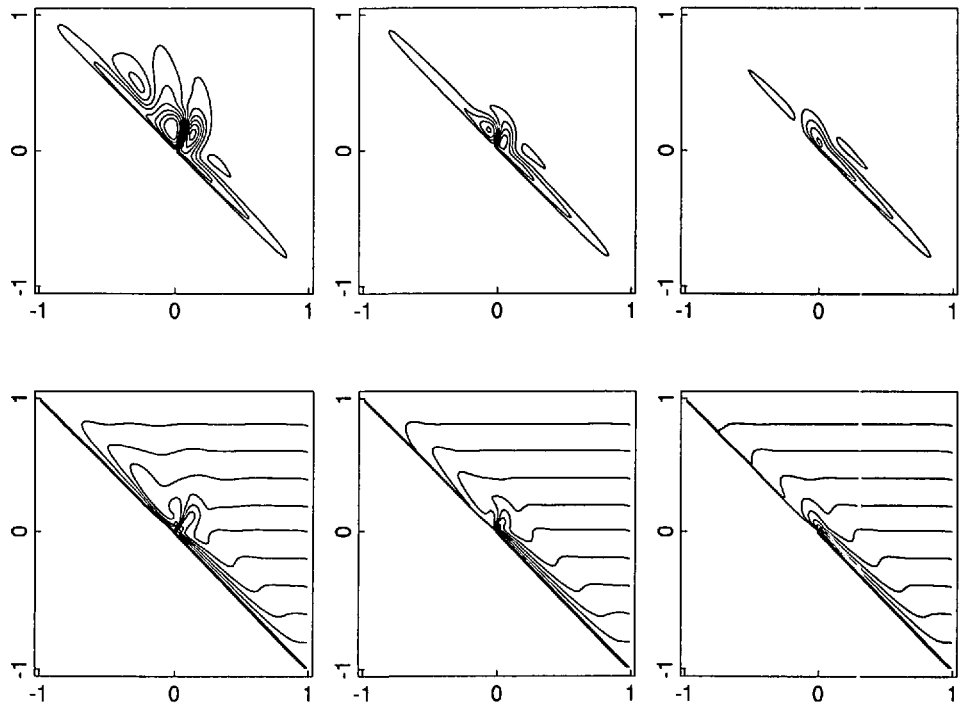

Figure 8. The streamfunction (contour interval 1×10^{-4}) and potential vorticity (contour interval 0.2) for a northwestward orientated coastline and a number of boundary forcing combinations. In each case the diffusivity was $K = 0.5 \times 10^{-4}$ and the forcing in the southern half of the basin $\xi = -1.0$. The forcing in the north was (a) $\xi = 1.0$, (b) $\xi = 0.5$ and (c) $\xi = 0.2$. The entire basin is shown, however the coastline has been omitted in the top figures so as not to obscure the streamlines.

The results described in this section indicate that inertial separation requires a region of coastal cyclonic relative vorticity. This can be understood quite simply in terms of geostrophy. The cyclone introduces a low pressure region against the western boundary. In order for the northward flow to remain near a geostrophic balance, it must keep this low pressure zone to its left. If the cyclonic region extends beyond the boundary layer, then geostrophy can only be maintained through complete separation of the northward flow.

6. Relevance to the North Brazil Current

Despite the very simplistic nature of the model, the flow patterns do suggest that certain aspects of the dynamics of the NBC have been well represented. Comparison of the flow pattern derived from observations in Figure 1 with the model run in Figure 8b, indicates that the appropriate velocity and length scales are produced by forcing in the south corresponding to $\xi \approx -1$ (as suggested by observations) and

forcing in the north corresponding to $\xi \approx 0.4$. The latter is equivalent to cyclonic vorticity of around $8 \times 10^{-6} s^{-1}$, which for a coastal cyclone of radius 70 km gives a realistic velocity scale of 0.6 m $s.^{-1}$. Slightly smaller values of ξ are appropriate for modeling the boreal winter flow.

The model explicitly assumes the distribution of relative vorticity in the boundary currents without explaining it origin. The source of the anticyclonic vorticity in the NBC is quite clearly equatorial water carried north over the planetary vorticity gradient. The source of the cyclonic vorticity which forms the observed coastal cyclone is less certain. In a classical subtropical-subpolar gyre system, the cyclonic vorticity may be produced as fluid travels southward in the western boundary current of the subpolar gyre. In the case of the Gulf Stream, there is a local cyclonic wind stress, while at subthermocline levels topography may create additional cyclonic vorticity (Hogg and Stommel, 1985). In contrast, the western boundary currents in the tropical and subtropical regions are both northward, producing only anticyclonic vorticity, and there is no evidence of cyclonic wind stress.

The only remaining source of cyclonic vorticity seems to be the western side of the NBC itself, where there is cyclonic shear vorticity (see for example the velocity sections of Flagg *et al.,* 1986). The curvature of the shelf break toward the west around 8N, may allow this vorticity to somehow "roll-up" to form the coastal cyclone. The details of this process are unclear, although there may be some analogy with the flow reversals of classical boundary layer separation. In any case, the potential importance of cyclonic vorticity on the western side of the current may help explain why the sophisticated primitive equation model of Philander and Pacanowski (1986) failed to produce the coastal cyclone. In particular, their grid spacing was probably too large to resolve this high shear region.

7. Conclusion

A simple one and a half layer quasi-geostrophic model has been used to study the separation and recirculation of western boundary currents. The only forcing applied to the flow was anomalous potential vorticity along the western boundary of the basin, which was allowed to diffuse into the fluid. Over most of the parameter range, this created a Munk type boundary layer governed by an inertial-diffusive balance (relation 20). For strong forcing or small diffusion, recirculation zones formed in which potential vorticity was approximately conserved. Evidence suggests that the sizes of these regions scaled in accordance with relation (25), which in all cases considered was much smaller than the predictions of one-dimensional theory. Nearly all streamlines passed through the western boundary layer and subsequently there was no observable homogenization of potential vorticity. Comparisons with the NBC and Demerara Anticyclone flow field show a good correspondence when realistic forcing is used in the model.

Another notable feature in the model, was the ability of a coastal cyclone

extending beyond the diffusive boundary layer to induce separation of the boundary current. It seems likely that this is a factor in the separation of the NBC. Csanady (1985) postulated that the NBC separates because it encounters fluid of higher potential vorticity. Our results imply that the higher potential vorticity must be associated with substantial cyclonic relative vorticity. This mechanism may also be relevant to other western boundary currents. For example, Boland and Church (1981) hypothesized that large excursions ($\sim$500 km) in the separation point of the East Australia Current can be induced by collisions with moving cyclonic eddies. Ierley (1990) also noted evidence of such events in recent eddy resolving numerical experiments. Further observations may reveal this to be a common feature of separating western boundry currents.

Acknowledgments. My thanks to Dr. G. T. Csanady for useful discussions on the problem and to an anonymous reviewer for valuable comments. This research was supported by the National Science Foundation under a grant entitled: The North Brazil Current: Its role in the equatorial heat and mass balance.

REFERENCES

Boland, F. M. and J. A. Church. 1981. The East Australia Current 1978. Deep-Sea Res., *28A,* 937–957.

Bruce, J. G. and J. L. Kerling. 1984. Near equatorial eddies in the North Atlantic. Geophys. Res. Lett., *11,* 779–882.

Cessi, P. 1988. A stratified model of the inertial recirculation. J. Phys. Oceanogr., *18,* 662–682.

—— 1990. Recirculation and separation of boundary currents. J. Mar. Res., *48,* 1–35.

Cessi, P., G. Ierley and W. Young. 1987. A model of the inertial recirculation driven by potential vorticity anomalies. J. Phys. Oceanogr., *17,* 1640–1652.

Csanady, G. T. 1985. A zero potential vorticity model of the North Brazilian Coastal Current. J. Mar. Res., *43,* 553–579.

—— 1987. What controls the rate of equatorial warm water mass formation. J. Mar. Res., *45,* 513–532.

—— 1990. Retroflection and leakage in the North Brazil Current: Critical point analysis. J. Mar. Res., *48,* 701–728.

Flagg, C. N., R. L. Gordon and S. McDowell. 1986. Hydrographic and current observations on the continental slope and shelf of the western equatorial Atlantic. J. Phys. Oceanogr., *16,* 1412–1429.

Hogg, N. G. and H. Stommel. 1985. On the relation between the deep circulation and the Gulf Stream. Deep-Sea Res., *32,* 1181–1193.

Ierley, G. R. 1990. Boundary layers in the general ocean circulation. Ann. Rev. Fluid Mech., *22,* 111–142.

Ierley, G. and W. Young. 1983. Can the western boundary layer affect the potential vorticity distribution in the Sverdrup interior of a wind gyre? J. Phys. Oceanogr., *13,* 1753–1763.

—— 1988. Inertial recirculation on a β-plane corner. J. Phys. Oceanogr., *18,* 683–689.

Marshall, J. C. and G. Nurser. 1986. Steady free circulation in a quasi-geostrophic ocean. J. Phys. Oceanogr., *16,* 1799–1813.

Merle, J. and S. Arnault. 1985. Seasonal variability of the surface dynamic topography in the tropical Atlantic Ocean. J. Mar. Res., *43,* 267–288.

Molinari, R. L. 1983. Observations of near-surface currents and temperatures in the central and western tropical Atlantic Ocean. J. Geophys. Res., *88,* 4433–4438.
Muller-Karger, F. E., C. R. McClain and P. L. Richardson. 1988. The dispersal of the Amazons water. Nature, *333,* 56–59.
Munk, W. H. 1950. On the wind-driven ocean circulation. J. Meteorol., *7,* 79–93.
Ou, H. S. and W. P. M. de Ruijter. 1986. Separation of an inertial boundary current from a curved coastline. J. Phys. Oceanogr., *16,* 280–289.
Parsons, A. T. 1969. A two layer model of Gulf Stream separation. J. Fluid Mech., *39,* 511–528.
Philander, S. G. H. and P. Delecluse. 1983. Coastal currents in low latitudes (with application to the Somali and El Nino currents). Deep-Sea Res., *30,* 887–902.
Philander, S. G. H. and R. C. Pacanowski. 1986. A model of the seasonal cycle in the tropical Atlantic Ocean. J. Geophys. Res., *91,* 14192–14206.
Rhines, P. B. and W. R. Young. 1982. Homogenization of potential vorticity in planetary gyres. J. Fluid Mech., *122,* 347–367.
Richardson, P. L. and T. K. McKee. 1984. Average seasonal variation of the Atlantic North Equatorial Countercurrent from ship drift data. J. Phys. Oceanogr., *14,* 1226–1238.
Richardson, P. L. and S. G. H. Philander. 1987. The seasonal variations of surface currents in the tropical Atlantic Ocean: A comparison of ship drift data with results from a general circulation model. J. Geophys. Res., *92,* 715–724.
Richardson, P. L. and G. Reverdin. 1987. Seasonal cycle of velocity in the Atlantic North Equatorial Countercurrent as measured by surface drifters, current meters, and ship drifts. J. Geophys. Res., *92,* 3691–3708.
Veronis, G. 1973. Model of world ocean circulation: 1 Wind-driven, two-layer. J. Mar. Res., *31,* 228–288.

Received: *10 July, 1990;* revised: *16 November, 1990.*